

Supporting information

Tuning Transport Properties in Thermoelectric Nanocomposites through Inorganic Ligands and Heterostructured Building Blocks

Maria Ibáñez,^{#,†,‡,} Aziz Genç,[§] Roger Hasler,^{†,‡} Yu Liu,[#] Oleksandr Dobrozhan,[⊥] Olga Nazarenko,^{†,‡} María de la Mata,[§] Jordi Arbiol,^{§¶} Andreu Cabot,^{⊥¶} and Maksym V. Kovalenko^{†,‡,*}*

AUTHOR ADDRESS

[#] Institute of Science and Technology Austria, Am Campus 1, 3400 Klosterneuburg, Austria

[†] Institute of Inorganic Chemistry, Department of Chemistry and Applied Biosciences, ETH Zürich, Vladimir Prelog Weg 1, CH-8093, Switzerland

[‡] Empa-Swiss Federal Laboratories for Materials Science and Technology, Dübendorf, Überlandstrasse 129, CH-8600, Switzerland

[§] Catalan Institute of Nanoscience and Nanotechnology (ICN2), CSIC and The Barcelona Institute of Science and Technology (BIST), Campus UAB, Bellaterra, 08193 Barcelona, Catalonia, Spain.

[⊥] Catalonia Energy Research Institute - IREC, Sant Adria del Besos, 08930 Barcelona, Spain

[¶] ICREA, Pg. Lluís Companys 23, 08010 Barcelona, Spain

* mibanez@ist.ac.at; mvkovalenko@ethz.ch

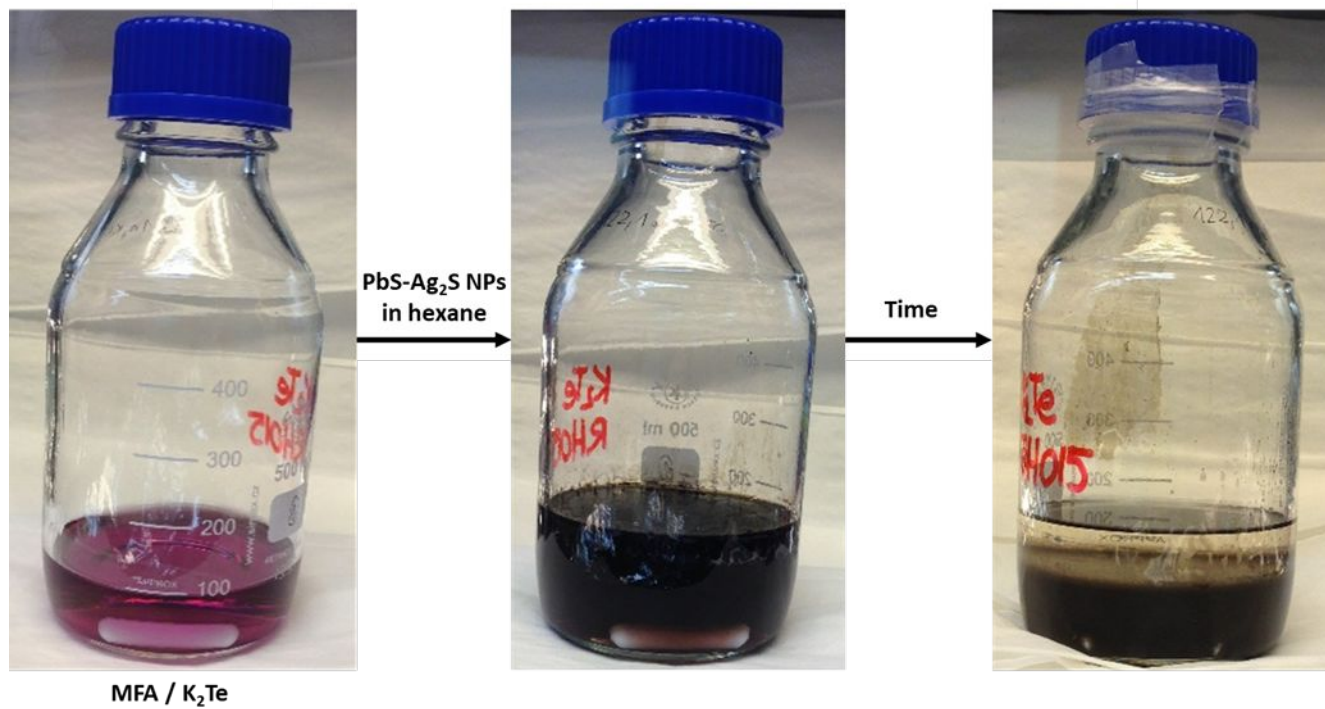


Figure S1. Pictures of the different steps of the large scale ligand exchange procedure with K_2Te in PbS- Ag_2S Nanorods.

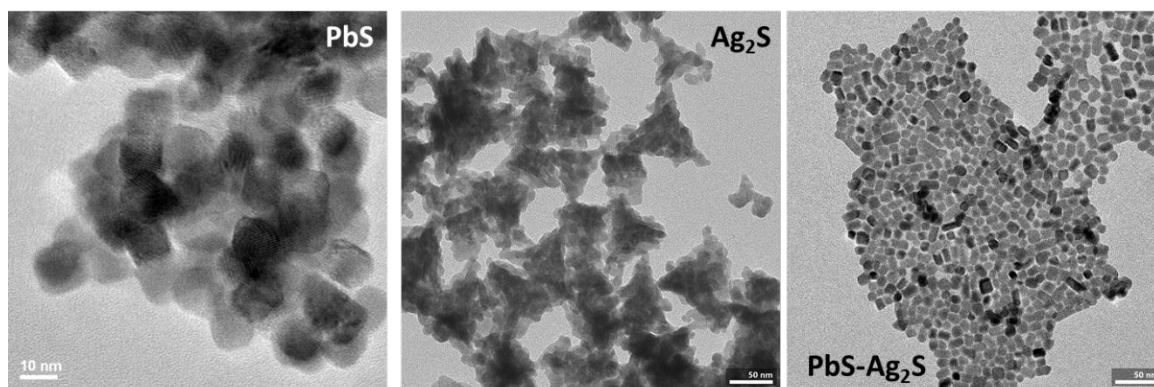


Figure S2. TEM image of the K_2Te surface functionalized NPs

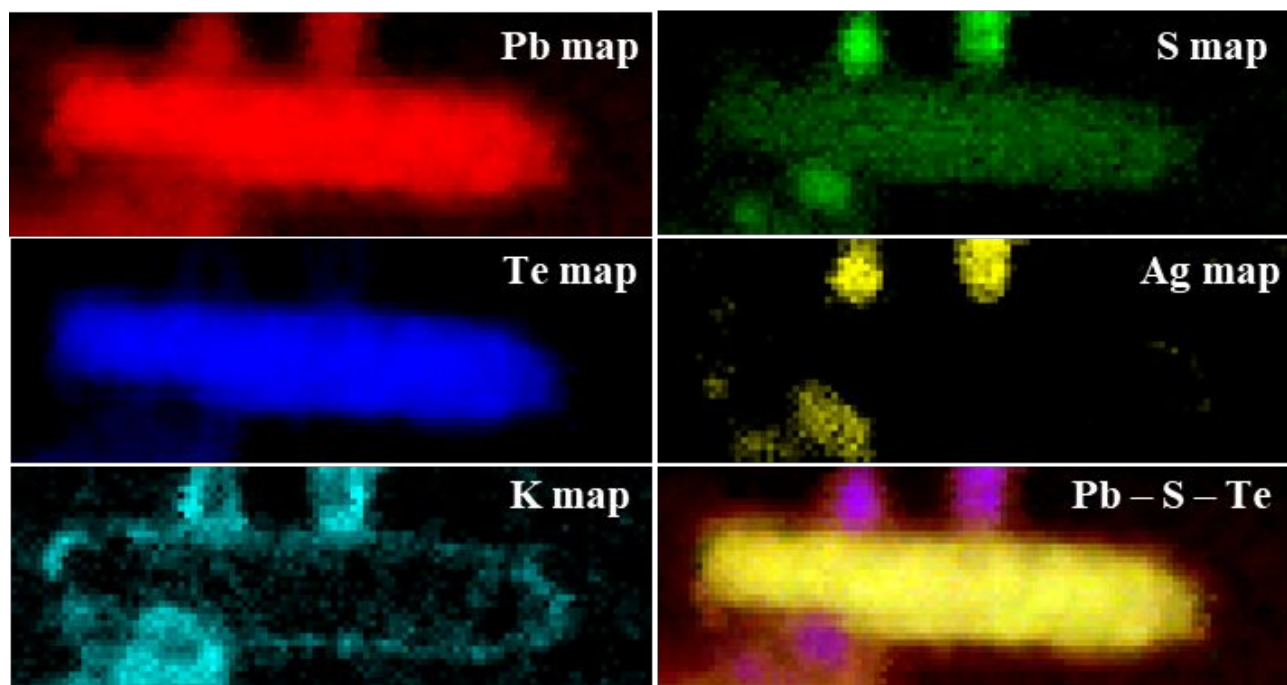


Figure S3. ADF STEM micrograph of two nanorods and several nanoparticles. STEM – EELS elemental composition maps: Pb (red), S (green), Te (blue), Ag (yellow) and K (turquoise) and composite image including Pb – S – Te. As can be seen from the elemental maps, Te generated from K_2Te is located at the main body of the nanorod with a quite homogeneous distribution, whereas K is mainly located at the surfaces of the nanorod and the nanoparticles. Nanoparticles located around the nanorod can be identified as silver sulfides (the reason we are not saying Ag_2S is that we cannot define the phase here) with some presence of Pb. The composite map of Pb, S and Te shows these 3 elements distributed fairly homogeneously throughout the nanorod. It should be noted here that the Pb map is obtained from the N6,7 edge located at 138 eV, rather than the typical M4,5 edge located at 2484 eV.

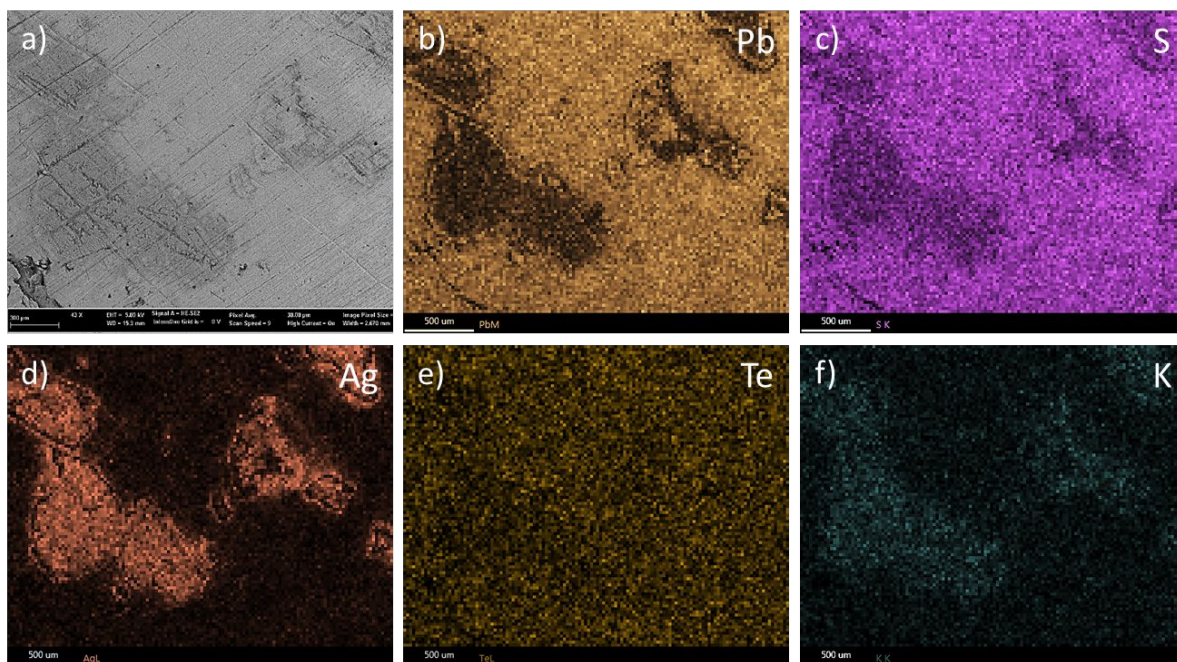


Figure S3. SEM image and elemental maps of the pellet produced by blending K_2Te surface modified PbS and Ag_2Te NPs.

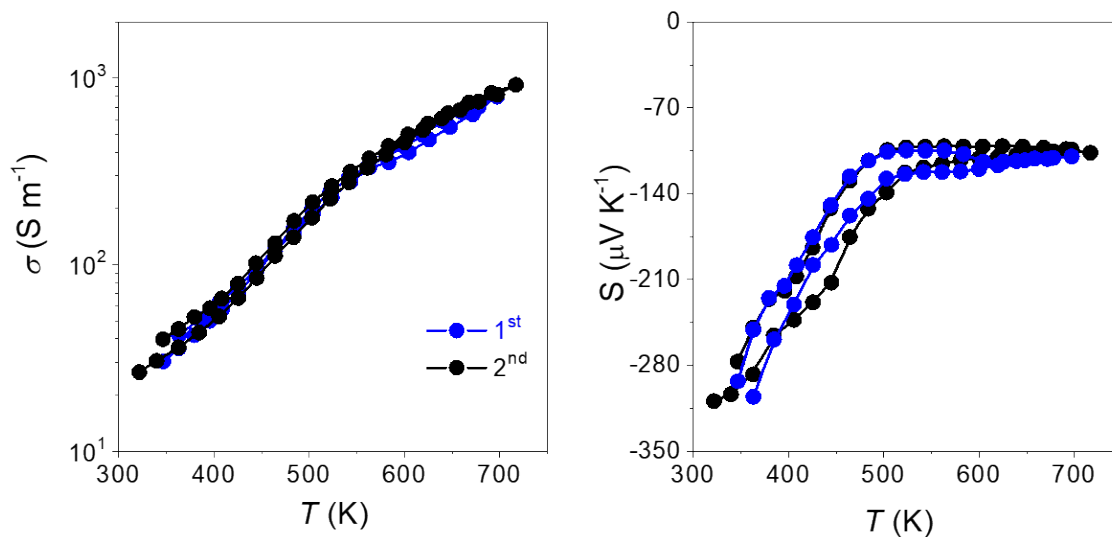


Figure S4. Electrical conductivity (left); Seebeck coefficient (centre) and power factor (right) of the nanocomposite made by blending K_2Te surface modified PbS and Ag_2Te NPs.

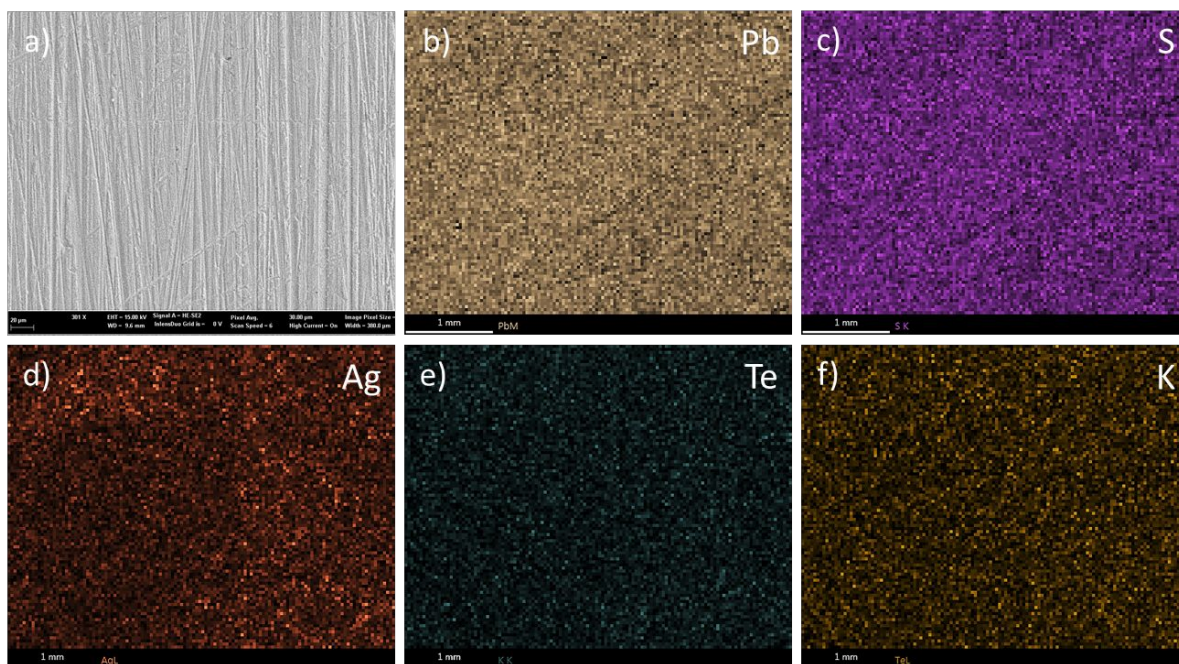


Figure S4. SEM image and elemental maps of the pellet produced by blending K_2Te surface modified PbS and Ag_2Te NPs

Table S1. Crystal domain size estimation using Scherrer equation and the XRD patterns.

	PbS	PbTe
PbS- Ag_2S - K_2Te NRs	11 nm	n.a.
PbS- Ag_2S - K_2Te powder	26 nm	29 nm
PbS- Ag_2S - K_2Te HP	40 nm	40 nm

Table S2. Heat capacity values used to calculate the thermal conductivity of the different nanomaterials presented in the manuscript. The heat capacity was calculated using the Dulong-Petit limit, taking into account the different phases of the nanocomposites and their content considering no alloying/doping. It is worth to mention that this calculation is in principle an upper limit if we consider that part of the Ag present is alloyed. However the difference is around 1-3% for the maximum possible content of Ag dissolved Pb chalcogenides (which we estimate to be below 2% based on previous works; J. Phys. D: Appl. Phys. 47, 115303, (2014)).

Nanomaterial	Heat capacity ($J g^{-1} K^{-1}$)
Pb-S	0.208
Pb-Ag-S	0.217
Pb-Ag-K-S-Te	0.199
Pb-K-S-Te	0.190

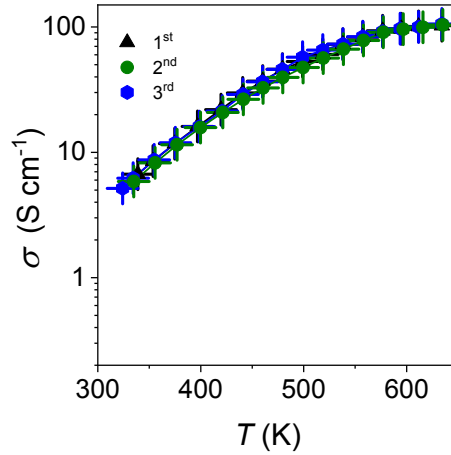


Figure S5. Temperature dependence of the electrical conductivity of $\text{Pb}_{0.81}\text{Ag}_{0.16}\text{K}_{0.03}\text{Te}_{0.33}\text{S}_{0.67}$ nanocomposite measured for 3 consecutive temperature cycles up 640 K

Table S3. Hall charge carrier concentration and mobility measured at ambient temperature.

$\text{Pb}_{0.81}\text{Ag}_{0.16}\text{K}_{0.03}\text{Te}_{0.33}\text{S}_{0.67}$	$p = 1 \times 10^{19} \text{ cm}^{-3}$	$\mu = 3.0 \text{ cm}^2 \text{ V}^{-1} \text{ s}^{-1}$
$\text{Pb}_{0.89}\text{Ag}_{0.10}\text{K}_{0.01}\text{Te}_{0.28}\text{S}_{0.72}$	$P = 8 \times 10^{18} \text{ cm}^{-3}$	$\mu = 0.6 \text{ cm}^2 \text{ V}^{-1} \text{ s}^{-1}$

Hole mobilities in similar p-type Pb chalcogenides produced by solid state are generally between 100 and 250 $\text{cm}^2/(\text{V}\cdot\text{s})$ at room temperature (J. Am. Chem. Soc., 2011, 133, 16588–16597; Nat. Commun. 2014, 5, 4515) . Approximately 2 orders of magnitude larger than our material. We associate this to the lower density of our material and the high concentration of grain boundary barriers.